Estimation of Quarticity with High Frequency Data*

Maria Elvira Mancino† and Simona Sanfelici‡

January 18, 2012

Abstract

We propose a new methodology based on Fourier analysis to estimate the fourth power of volatility function (spot quarticity) and, as a byproduct, the integrated function. We prove consistency of the proposed estimator of integrated quarticity. Further we analyze its efficiency in the presence of microstructure noise, both from a theoretical and empirical viewpoint. Extensions to higher powers of volatility and to the multivariate case are also discussed.

JEL: G10, C13, C14, C58.
Keywords: volatility, covariance, quarticity, microstructure, Fourier analysis.

1 Introduction

In the last decade many empirical and theoretical studies have shown that using high frequency intradaily returns allows to get more efficient measures of volatility than classical estimates obtained through daily data. Nevertheless, the efficiency of all the methodologies proposed in accurately estimating the volatility must cope with the fact that observed asset prices are contaminated by market microstructure effects, such as price discreteness, separate trading prices for buyers and sellers and other contaminations; as a consequence, observed asset prices diverge from their efficient values and any volatility measure is rapidly swamped by noise [Roll, 1984]. Different methods have been proposed to obtain unbiased estimators of the true integrated volatility, e.g. [Zhou, 1996, Andersen et al., 2001, Zhang et al., 2005, Mancino and Sanfelici, 2008, Barndorff-Nielsen et al

In order to produce feasible central limit theorems for all these estimators, and hence feasible confidence intervals, it is necessary to obtain efficient estimators of the so called *quarticity*, which appears as conditional variance in the central limit theorems. Nevertheless, the studies about estimation of quarticity are still few. In fact, [Barndorff-Nielsen et al., 2008a] remark that *estimating integrated quarticity reasonably efficiently is a tougher problem than estimating the integrated volatility*, as the effect of noise is magnified up. [Barndorff-Nielsen and Shephard, 2004a, Barndorff-Nielsen et al., 2006] proposed an estimator of quarticity which is consistent in the absence of noise; this is the mostly used estimator of quarticity and sparse sampling is usually employed to face microstructure noise problems (see also [Bandi and Russell, 2006]). Finally, [Mykland, 2007] proposed an improved estimator of quarticity, based on a local pre-averaging

*We wish to thank Neil Shephard, Dobrislav Dobrev, Frederi Viens and an anonymous referee for their insightful comments and remarks.

†DiMaD, University of Firenze, Italy, mariaelvira.mancino@dmd.unifi.it

‡Dept. of Economics, University of Parma, Italy, simona.sanfelici@unipr.it

technique, which generalizes the estimator by [Barndorff-Nielsen and Shephard, 2002]. However, the issue of microstructure effects is not considered. [Schulz, 2010] proposes an approach to robustify any estimator in order to cope with flat prices and no trading, both frequently occurring stylized facts in financial high-frequency data sets, which can cause a considerable bias in each considered method. Very recently, [Andersen et al., 2011] provide an in-depth look at robust estimation of integrated quarticity based on high frequency data, document the empirical challenges posed by data sampling imperfections and propose a new family of neighborhood truncation estimators, that generalizes existing nearest neighbor estimators based on the minimum of two adjacent absolute returns or on the median of three adjacent absolute returns. These estimators perform very well in the presence of jumps but are less efficient for diffusive processes.

In this paper we propose a new method to estimate quarticity, which is based on the Fourier volatility estimation proposed in [Malliavin and Mancino, 2002]. The Fourier methodology allows to reconstruct the *instantaneous volatility* as a series expansion with coefficients gathered from the Fourier coefficients of the price variation. The consistency in probability uniformly in time and the asymptotic properties of the Fourier estimator of instantaneous volatility have been proved in [Malliavin and Mancino, 2009] in the absence of microstructure noise. Moreover the efficiency of the Fourier method to estimate the integrated volatility in the presence of microstructure noise has been analyzed in comparison with other estimators in [Mancino and Sanfelici, 2008]. The authors find that the Fourier estimator needs no correction in order to be statistically efficient and robust to some kind of market frictions at the same time. This result is due to the following properties of the Fourier estimator: on one side it uses all available data by integration, therefore incorporating not only the squared increments of the prices but also the auto-covariances of all orders along the time window; on the other side the high-frequency noise or short-run noise is ignored by cutting the highest frequencies in the construction of the estimator.

In order to construct an estimator of quarticity we employ the Fourier coefficients of volatility obtained through the Fourier methodology in [Malliavin and Mancino, 2009] and the product formula. Note that our methodology allows to compute the fourth power of volatility function (*spot quarticity*) and not only the integrated function. We compute analytically the mean square error (MSE) of the Fourier estimator of quarticity and prove its consistency in the absence of noise. In the presence of microstructure effects, we propose an efficient corrected Fourier estimator which has lower sensitivity to the noise component. Further we address the problem of constructing an optimal MSE-based Fourier quarticity estimator, which renders our methodology feasible with real data on finite samples. In fact, when using high frequency data, the efficiency of the Fourier estimator largely depends on the choice of two parameters M and N, which define the highest frequency Fourier coefficients taken into account by the estimator.

The new methodology is tested in realistic Monte Carlo experiments and in an empirical application to S&P 500 index futures. We make a comparative analysis of the performance of most of the estimators existing in the literature. Our analysis shows that a very attractive feature of the Fourier methodology is its ability to cope with microstructure effects. More precisely, our estimator is robust to increasing noise effects as a consequence of its property of ignoring high-frequency noise components by cutting the highest frequencies of the observed process.

The paper is organized as follows. In Section 2 the computation of the quarticity function through Fourier analysis is proposed. Section 3 proves the consistency of the Fourier quarticity estimator. In Section 4 the properties of the Fourier quarticity estimator in the presence of microstructure noise are analyzed. Extension to the multivariate case is sketched in Section 5. Section 6 contains the simulation results and an application to S&P 500 index futures. Section

7 concludes. The technical proofs are contained in the Appendix.

2 Computation of the fourth power of spot volatility

Let $p(t)$ be the logarithm of an asset price, observed at time t over a fixed time period (e.g. a trading day), say $[0,T]$. We assume $p(t)$ to be a continuous semi-martingale satisfying the stochastic differential equation

$$(\mathbf{A.I}) \qquad dp(t) = \sigma(t)\, dW(t) + b(t)\, dt,$$

where W is a Brownian motion on a filtered probability space $(\Omega, (\mathcal{F}_t)_{t\in[0,T]}, P)$, σ and b are adapted stochastic processes such that

$$E[\int_0^T \sigma^8(t)dt] < \infty \quad , \quad E[\int_0^T b^4(t)dt] < \infty.$$

We aim at computing the fourth power of the volatility function $\sigma(t)$. To this end, we propose a methodology which allows to compute its Fourier coefficients from the asset prices observations and therefore to recover its Fourier expansion.

The Fourier method for spot variance estimation was first introduced in [Malliavin and Mancino, 2002]. In contrast with the realized volatility type estimators, the peculiarity of Fourier approach is that it allows to reconstruct the variance as a *stochastic function of time* in the univariate and multivariate case, not only the integrated variance. In this paper we will exploit this property: in fact by our methodology all the Fourier coefficients of the variance function can be obtained, which allows us to compute the fourth power of the volatility function, namely the *spot quarticity*. In the following, we will assume that, up to a translation and a scaling in time, the time window is $[0, 2\pi]$.

For any integer k, define the *Fourier transform* of dp by

$$\mathcal{F}(dp)(k) := \frac{1}{2\pi} \int_{]0,2\pi[} \exp(-\mathrm{i}kt)\, dp(t).$$

The first step of our method consists in the computation of the Fourier coefficients of the function $\sigma^2(t)$

$$\mathcal{F}(\sigma^2)(k) := \frac{1}{2\pi} \int_0^{2\pi} e^{-\mathrm{i}kt} \sigma^2(t) dt.$$

This can be obtained using the following result: the variance function is computed by establishing a connection between the Fourier transform of the price process and the Fourier transform of the variance process. This link is provided by the next theorem, which is proved in [Malliavin and Mancino, 2009]. For simplicity, we can assume $b = 0$ because the drift term gives no contribution to the estimation of the Fourier coefficients of the volatility (see [Malliavin and Mancino, 2009]).

Theorem 2.1 *Consider a semi-martingale p satisfying assumption* **(A.I)**. *The following convergence in probability holds*

$$\mathcal{F}(\sigma^2)(k) = \lim_{N\to\infty} \frac{2\pi}{2N+1} \sum_{|s|\le N} \mathcal{F}(dp)(s)\, \mathcal{F}(dp)(k-s), \quad \textit{for all } k \in \mathbf{Z}. \tag{1}$$

The second step consists in the computation of the k-th Fourier coefficient of $\sigma^4(t)$. To this end, the Fourier series of a product can be applied.

Proposition 2.2 *Under assumption* **(A.I)** *the k-th Fourier coefficient of the function* $\sigma^4(t)$ *is obtained as the following limit in probability*

$$\mathcal{F}(\sigma^4)(k) = \lim_{M\to\infty} \sum_{|s|\leq M} \mathcal{F}(\sigma^2)(s)\, \mathcal{F}(\sigma^2)(k-s). \tag{2}$$

Finally the fourth power of volatility function can be reconstructed by means of its Fourier coefficients (2) as the following limit in probability

$$\sigma^4(t) = \lim_{N\to\infty} \sum_{|k|<N} (1 - \frac{|k|}{N}) \mathcal{F}(\sigma^4)(k) \exp(\mathrm{i}kt) \quad \text{for all } t \in (0, 2\pi). \tag{3}$$

Remark 2.3 *The Fourier methodology presented in this section can be easily accommodated to obtain unbiased estimators of higher power function of volatility: in fact by using as building blocks the Fourier coefficients of the variance function and the product formula, we can compute the Fourier coefficients of any positive even power of the volatility function.*

Remark 2.4 *We observe that in particular it holds*

$$\int_0^{2\pi} \sigma^4(t)dt = 2\pi \mathcal{F}(\sigma^4)(0),$$

therefore the integrated quarticity can be obtained from equation (2) by setting $k = 0$.

We stress the point that in order to compute the quarticity, that is the integrated fourth power of volatility function, the knowledge of the integrated volatility is not sufficient, but (all) the Fourier coefficients of the volatility are needed. We will discuss again this issue in Remark 3.2.

3 Fourier estimator of quarticity

In this section an estimator of quarticity is constructed through a two steps procedure: firstly, given the discrete observations of the price process, an estimator of the Fourier coefficients of the spot variance process is obtained; secondly, using the product formula and the estimated Fourier coefficients of the variance process, we propose an estimator of quarticity.

Suppose that the asset log-price $p(t)$, satisfying assumption **(A.I)**, is observed at discrete, irregularly spaced points in time: $\{0 = t_{0,n} \leq \dots t_{i,n} \dots \leq t_{n,n} = 2\pi\}$. For simplicity we will omit the second index n. Denote $\rho(n) := \max_{0\leq h\leq n-1} |t_{h+1} - t_h|$ and suppose that $\rho(n) \to 0$ as $n \to \infty$.

Consider the following interpolation formula

$$p_n(t) := \sum_{i=0}^{n-1} p(t_i) I_{[t_i, t_{i+1}[}(t).$$

and denote the returns by $\delta_i(p) := p(t_{i+1}) - p(t_i)$. For any integer k, $|k| \leq 2N$, set

$$c_k(dp_n) := \frac{1}{2\pi} \sum_{i=0}^{n-1} \exp(-\mathrm{i}kt_i)\delta_i(p). \tag{4}$$

For any $|k| \leq N$, define

$$c_k(\sigma^2_{n,N}) := \frac{2\pi}{2N+1} \sum_{|s|\leq N} c_s(dp_n) c_{k-s}(dp_n) \tag{5}$$

as the discrete counterpart of (1). Finally define

$$\sigma^2_{n,N}(t) := \sum_{|k|<N} (1 - \frac{|k|}{N}) c_k(\sigma^2_{n,N}) e^{\mathrm{i}kt}. \tag{6}$$

The random function $\sigma^2_{n,N}(t)$ will be called the *Fourier estimator* of the instantaneous variance $\sigma^2(t)$.

In the sequel we will suppose that $\sigma(t)$ is a continuous function and satisfies:

$$(\mathbf{A}.\mathbf{II}) \qquad \operatorname{ess\,sup} \|\sigma^2\|_{L^\infty} < \infty, \quad \text{where } \|\sigma^2\|_{L^\infty} := \sup_t |\sigma^2(t)|.$$

The following result states the consistency of the Fourier estimator of instantaneous variance. The proof can be found in [Malliavin and Mancino, 2009].

Theorem 3.1 *(i) For any integer k, if $\rho(n)N \to 0$, then the following convergence in probability holds*

$$\lim_{n,N\to\infty} c_k(\sigma^2_{n,N}) = \mathcal{F}(\sigma^2)(k).$$

(ii) Further, it holds in probability

$$\lim_{n,N\to\infty} \sup_{t\in(0,2\pi)} |\sigma^2_{n,N}(t) - \sigma^2(t)| = 0.$$

Relying on Proposition 2.2 and Remark 2.4, we define the *Fourier estimator of quarticity* by

$$\sigma^4_{n,N,M} := 2\pi \sum_{|s|<M} (1 - \frac{|s|}{M}) c_s(\sigma^2_{n,N}) c_{-s}(\sigma^2_{n,N}), \tag{7}$$

where the $c_*(\sigma^2_{n,N})$ are explicit functions of the log-returns $\delta_i(p)$ $(i = 1, \ldots, n)$ as defined by (5). In (7) we have chosen the Fourier-Fejer summation by adding a Barlett kernel, which improves the behavior of the estimator for very high observation frequencies.

Remark 3.2 *Notice that when $M = 1$ the Fourier estimator of quarticity is simply the squared Fourier estimator of integrated volatility. Indeed, recognizing the considerable imprecision of quarticity estimators, other authors such as [Jiang and Oomen, 2008] opted for simply squaring integrated variance estimators. In this regard, higher order Fourier coefficients $c_s(\sigma^2_{n,N})$ for $s \geq 1$ contribute to increase the precision of the quarticity estimator with respect to that naive approach.*

The main result of this section is the following theorem which proves the consistency of estimator (7).

Theorem 3.3 *Let $\sigma^4_{n,N,M}$ be defined in (7). If $\rho(n)NM \to 0$ and $\frac{M^2}{N} \to 0$ as $M, N, n \to \infty$, then the following convergence in probability holds*

$$\lim_{n,N,M\to\infty} \sigma^4_{n,N,M} = \int_0^{2\pi} \sigma^4(t)dt.$$

This result establishes a link between the number of observations n and the parameters M, N. However, in practical situations the number of observations n is finite and fixed. In order to obtain a feasible finite sample estimator of the integrated quarticity, we compute analytically an upper bound for the MSE of the Fourier quarticity estimator. This result will provide a practical way to optimize the finite sample performance of the Fourier estimator as a function of the number of frequencies M and N by the minimization of the estimated mean squared error, for a given number of intra-daily observations n. Thus, it can be effectively used to build optimal MSE-based estimators.

Corollary 3.4 *Under assumptions* **(A.I)** *and* **(A.II)** *then*

$$E[|\sigma^4_{n,N,M} - \int_0^{2\pi} \sigma^4(t)dt|^2] \leq$$

$$\leq \frac{2^5\pi^2}{3} M^2 \operatorname{ess\,sup} \|\sigma^2\|^4_{L^\infty} \left(C_1^{1/2} \rho(n)^2 [N^2 + M^2] + \frac{C_2^{1/2}}{2N+1} \right) + (2\pi)^2 \operatorname{ess\,sup} \|\sigma^2\|^2_{L^\infty} (\omega_{\sigma^2}(\frac{4}{M}))^2,$$

where $C_1 = 2^6 \cdot 7$, $C_2 = 9 \cdot \frac{2^7}{\pi}$ *and* $\omega_{\sigma^2}(\lambda)$ *denotes the modulus of continuity of the variance function.*

4 Fourier quarticity estimator in the presence of noise

It is widely recognized that in the presence of microstructure noise the realized volatility estimator fails to converge to the integrated volatility of the underlying price process, e.g. see [Andersen and al., 1999]. Therefore, many ad hoc procedures have been proposed to correct the bias caused by the microstructure noise frictions. This problem is even magnified up when the integrated quarticity is estimated through the realized quarticity, which essentially involves the fourth order return moments.

The finite sample properties of the Fourier estimator of integrated volatility in the presence of market microstructure noise have been studied in [Mancino and Sanfelici, 2008], both in the case of independent noise and in the case where the noise is correlated with the efficient returns. In particular the authors find that, even without any bias correction of the estimator, the bias of a finite sample can be made negligible by suitably cutting the highest frequencies in the Fourier expansion. Moreover, they prove that the mean squared error of the Fourier estimator is substantially unaffected by the presence of microstructure noise by choosing in an appropriate way the number of Fourier coefficients to be included in the estimation, as indicated explicitly by the mean squared error computation.

In this section we claim the effectiveness of Fourier estimation method when applied to compute the quarticity in the presence of microstructure noise, due to the intrinsic robustness of the Fourier estimator of volatility.

Following a large literature in this field (e.g. [Hansen and Lunde, 2006]), we suppose that the logarithm of the observed price process is given by

$$\widetilde{p}(t) = p(t) + \eta(t), \tag{8}$$

where $p(t)$ is the efficient log-price process satisfying **(A.I)** and $\eta(t)$ is the microstructure noise. We can think of $p(t)$ as the log-price in equilibrium, that is the price that would prevail in the absence of market microstructure frictions.

We make the following assumptions:

(A.III) The random shocks $\eta(t_{j,n})$, for $0 \leq j \leq k_n$ and for all n, are independent and identically distributed with mean zero and bounded fourth moment.

(A.IV) The true return process $\delta_{j,n}(p) := p(t_{j+1,n}) - p(t_{j,n})$ is independent of $\eta(t_{j,n})$ for any j, n.

To simplify the notation, in the sequel we will write $\delta_j(p)$ and η_j instead of $\delta_{j,n}(p)$ and $\eta(t_{j,n})$ respectively. Denote $\delta_j(\tilde{p}) := \tilde{p}(t_{j+1}) - \tilde{p}(t_j)$, where $\tilde{p}$ is given in (8), and define $\varepsilon_j := \eta_{j+1} - \eta_j$ as the j-th noise return.

As in (7), the Fourier estimator of quarticity given noisy observations is given by

$$\widetilde{\sigma}^4_{n,N,M} := 2\pi \sum_{|s|<M} (1 - \frac{|s|}{M}) c_s(\widetilde{\sigma}^2_{n,N}) c_{-s}(\widetilde{\sigma}^2_{n,N}) \tag{9}$$

where the Fourier coefficients $c_s(\widetilde{\sigma}^2_{n,N})$ are now computed using Fourier methodology from the noisy returns $\delta_j(\tilde{p})$, namely

$$c_s(\widetilde{\sigma}^2_{n,N}) := \frac{2\pi}{2N+1} \sum_{|k|\leq N} c_k(d\tilde{p}_n) c_{s-k}(d\tilde{p}_n). \tag{10}$$

In the following theorem we investigate the asymptotic properties of the estimator (9). It turns out that the estimator is not consistent in its original form (9); nevertheless we compute the bias induced by the microstructure noise and we propose a correction which renders the Fourier estimator of quarticity more efficient in the presence of microstructure effects. As we will see in Section 6, this noise correction makes the estimator less sensitive to the choice of the parameter M and, in general, allows to use larger values of M, thus including in the expansion (9) a larger number of coefficients than in the uncorrected version. Nevertheless, we stress the fact that, although not consistent, the uncorrected estimator (9) is rather efficient as well, as it will be evident from the simulation results.

The definition of the Fourier estimator does not require evenly spaced data. Anyway for simplicity, in the following theorem we will suppose that the observations are equidistant in time and that $\rho(n) = 2\pi/n$ is the distance between two subsequent observations, where $[0, 2\pi]$ is the trading period.

Theorem 4.1 *Under the assumptions* **(A.I) - (A.IV)**, *then*

$$E[\widetilde{\sigma}^4_{n,N,M} - \ \sigma^4_{n,N,M}] = \Lambda_{n,N,M}(\sigma, \eta) + \Psi_{n,N,M}(\eta),$$

where $\widetilde{\sigma}^4_{n,N,M}$ *is defined in (9),* $\sigma^4_{n,N,M}$ *in (7),* $\Lambda_{n,N,M}(\sigma, \eta)$ *goes to* 0 *under the conditions* $\frac{MN^2}{n} \to 0$ *and* $\frac{M^3}{N} \to 0$, *as* $n, N, M \to \infty$, *and*

$$\Psi_{n,N,M}(\eta) = \frac{2}{\pi}(E[\eta^4] + 3E[\eta^2]^2) nM D^2_N(\frac{2\pi}{n}), \tag{11}$$

with $D_N(t)$ *denoting the rescaled Dirichlet kernel defined by*

$$D_N(t) := \frac{1}{2N+1} \frac{\sin[(N + \frac{1}{2})t]}{\sin \frac{t}{2}}. \tag{12}$$

Remark 4.2 *The growth conditions needed in Theorem 4.1 imply the two conditions* $NM\rho(n) \to 0$ *and* $\frac{M^2}{N} \to 0$ *required to ensure consistency of the estimator in the absence of noise.*

In order to obtain feasible optimal estimators it is useful to have the explicit expression for the asymptotically vanishing term $\Lambda_{n,N,M}(\sigma,\eta)$:

$$\Lambda_{n,N,M}(\sigma,\eta) = \alpha_{n,N,M}(\sigma,\eta) + n\ \beta_{n,N,M}(\sigma,\eta) + n^2\ \gamma_{n,N,M}(\eta), \tag{13}$$

where

$$\alpha_{n,N,M}(\sigma,\eta) = \operatorname{ess\,sup} \|\sigma^2\|_{L^\infty}\ 8\ E[\eta^2]\ \left(M(1-V_M(\frac{2\pi}{n})) + MV_M(\frac{2\pi}{n})(1-D_N(\frac{2\pi}{n}))\right) + o(1),$$

$$\beta_{n,N,M}(\sigma,\eta) = \operatorname{ess\,sup} \|\sigma^2\|_{L^\infty}\ 8\ E[\eta^2] \left(\frac{2}{\pi}\ \frac{M}{2N+1}(1-V_M(\frac{2\pi}{n})) + \frac{1}{4\pi}(1-D_N(\frac{2\pi}{n}))\right) +$$

$$+\frac{1}{\pi}(E[\eta^4]+3E[\eta^2]^2)\left(M(1-V_M(\frac{2\pi}{n})) + 2MV_M(\frac{2\pi}{n})(1-D_N(\frac{2\pi}{n}))\right) + o\left(\frac{1}{n}\right),$$

$$\gamma_{n,N,M}(\eta) = \frac{1}{\pi}E[\eta^2]^2\left((1-D_N(\frac{2\pi}{n}))^2 + 8\frac{M}{2N+1}(1-V_M(\frac{2\pi}{n}))\right),$$

where $V_M(t)$ is the Fejer kernel defined as $V_M(t) := (\frac{\sin Mt}{Mt})^2$.

We observe that term (11) is equal to $\frac{1}{\pi}E[\varepsilon^4]nMD_N^2(\frac{2\pi}{n})$. In [Bandi and Russell, 2005] it is proved that $\frac{1}{n}\sum_{j=1}^n \delta_j(\tilde{p})^4$ is a consistent estimator of the fourth moment of the noise $E[\varepsilon^4]$ as $n \to \infty$. Thus we correct the Fourier estimator of quarticity as follows

$$\hat{\sigma}^4_{n,N,M} := \widetilde{\sigma}^4_{n,N,M} - \hat{\Psi}_{n,N,M}, \tag{14}$$

where we have defined

$$\hat{\Psi}_{n,N,M} := \frac{M}{\pi}D_N^2(\frac{2\pi}{n})\sum_{j=1}^n \delta_j(\tilde{p})^4.$$

We call (14) the *corrected Fourier estimator*. We remark that (14) is still not consistent in the presence of noise, but less biased, as it will be confirmed in the numerical applications of Section 6.

5 Multivariate extension

The Fourier method was originally proposed in [Malliavin and Mancino, 2002] for estimating multivariate volatility in order to overcome the difficulties arising by applying the quadratic covariation formula to the true return data, due to the non-synchronicity of observed prices for different assets. In fact, the quadratic covariation formula is not well suited to provide a good estimate of cross-volatilities, because it requires synchronous observations, while in reality they are not available. The non-synchronicity trading problem has been studied for quite a long time in empirical finance, e.g. [Lo and MacKinlay, 1990]. The bias (*Epps effect*) caused by non-synchronicity and random sampling for the cross-correlations estimation has been recently highlighted in [Renó, 2003, Hayashi and Yoshida, 2005, Zhang, 2006].

The Fourier methodology is immune from these difficulties due to its own definition since, being based on the integration of "all" data for each asset prices, it does not need any adjustment

to fit to asynchronous observations. Thus we can extend without essential changes the univariate theory proposed in the previous sections, in order to obtain a high frequency estimator of the multivariate counterpart of quarticity. To the best of our knowledge, the only paper which proposes a consistent estimator of multivariate quarticity is [Barndorff-Nielsen and Shephard, 2004b], where the issue of microstructure noise and asynchronicity is not considered.

For simplicity, we illustrate the methodology in the bivariate case. Assume that $p(t) = (p^1(t), p^2(t))$ are Brownian semi-martingales satisfying Itô stochastic differential equations

$$dp^j(t) = \sum_{i=1}^{d} \sigma_i^j(t)\ dW^i + b^j(t)\ dt, \qquad j = 1, 2, \tag{15}$$

where W^1, W^2 are independent Brownian motions, and σ_*^* and b^* are adapted random processes satisfying hypothesis (**A**.**I**).

From the representation (15) define the *volatility matrix*, which in our hypothesis *depends upon time*, whose entries are

$$\Sigma^{jk}(t) = \sum_{i=1}^{d} \sigma_i^j(t)\sigma_i^k(t) \qquad j, k = 1, 2. \tag{16}$$

We show how to obtain an estimator of the *bivariate quarticity*, namely

$$\int_0^{2\pi} [\Sigma^{11}(t)\Sigma^{22}(t) + (\Sigma^{12}(t))^2]dt.$$

Our theory contains the general result: in the first step the Fourier coefficient of Σ^{ij} are computed by means of the following convergence in probability, which is proved in [Malliavin and Mancino, 2009]

$$\mathcal{F}(\Sigma^{ij})(k) = \lim_{N\to\infty} \frac{2\pi}{2N+1} \sum_{s=-N}^{N} \mathcal{F}(dp^i)(s)\mathcal{F}(dp^j)(k-s) \qquad \text{for any integer } k.$$

Once the Fourier coefficients of the functions Σ^{ij} have been estimated, the product formula contained in Proposition 2.2 applies.

By virtue of the efficiency properties of the covariance Fourier estimator even in the presence of microstructure noise, which has been investigated in [Mancino and Sanfelici, 2010], we expect a good performance of the multivariate version of Fourier quarticity estimator.

6 Empirical Analysis

We conduct realistic Monte Carlo experiments aiming to compare the performance of the Fourier quarticity estimator and of most of the estimators existing in the literature. Finally, we show an empirical application to S&P 500 index futures.

6.1 Numerical simulations

In this section we simulate discrete data from a continuous time stochastic volatility model with and without microstructure contaminations. From the simulated data, Fourier estimates of the integrated quarticity can be compared to the value of the true quantity and to estimates obtained with other methods proposed in the literature. To our best knowledge, although

the fourth power of volatility has many important applications in Econometrics, only very recently the literature has been focused specifically on the analysis of estimators for integrated quarticity [Andersen et al., 2011, Schulz, 2010, Mykland, 2007]. For the reader's convenience, in the following we recall the main integrated quarticity estimators that can be drawn from the literature.

[Barndorff-Nielsen and Shephard, 2002] provide an estimator of the integrated quarticity that is consistent in the absence of microstructure frictions

$$RQ := \frac{n}{3T}\sum_{i=0}^{n-1}\delta_i(p)^4.$$

To obtain roughly unbiased and valid estimates of quarticity when microstructure effects play a role, we can resort to low frequency sampling. To reduce the estimation error, [Ghysels and Sinko, 2007] combine the realized quarticity estimator with the averaging over subsamples approach proposed by [Zhang et al., 2005], where the returns span several ticks. While less efficient in the absence of noise, it reduces the variance due to noise and has a bias reducing effect. This estimator can be written as

$$RQ_{sub} := \frac{1}{S}\sum_{s=1}^{S} RQ^{(s)},$$

where the $RQ^{(s)}$'s are computed on different non overlapping subgrids using only the skip-S returns for the asset. Alternatively, the integrated quarticity may be estimated from the *bipower variation* measure of [Barndorff-Nielsen and Shephard, 2004a]

$$BQ := \frac{n}{T}\sum_{i=1}^{n-1}|\delta_i(p)|^2|\delta_{i-1}(p)|^2. \tag{17}$$

In [Barndorff-Nielsen and Shephard, 2004b] a possible combination of power and bipower quarticity is provided

$$Q := \frac{n}{2T}\left(\sum_{i=0}^{n-1}\delta_i(p)^4 - \sum_{i=1}^{n-1}|\delta_i(p)|^2|\delta_{i-1}(p)|^2\right).$$

[Barndorff-Nielsen et al., 2008a] propose a subsampled version of the bipower quarticity (17), which can be defined as follows. For some $\tilde{h} > 0$, define the subsampled squared returns $x_j^2 = \frac{1}{S}\sum_{s=0}^{S-1}\left(p_{\tilde{h}(j+\frac{s}{S})} - p_{\tilde{h}(j-1+\frac{s}{S})}\right)^2$, $j = 1, 2, \ldots, \tilde{n}$, where $\tilde{n} = \lfloor T/\tilde{h}\rfloor$. The subsampled bipower quarticity estimator may be given by

$$BQ_{sub} := \frac{T}{\tilde{n}}\sum_{j=1}^{\tilde{n}}\tilde{h}^{-2}(x_j^2 - 2\omega^2)(x_{j-2}^2 - 2\omega^2),$$

where $\omega^2 = Var(\eta_t)$. Detailed calculations show that for large S and small $\tilde{h}$ the conditional variance of BQ_{sub} is approximately $72\omega^8\tilde{n}^3/S^2$, so that $\tilde{h}^{3/2}S \to \infty$ leads to consistency.

A possible generalization of the realized bipower variation measure can be obtained by summing products of adjacent absolute returns raised to powers less than two, as in, e.g., the following standardized *realized tripower quarticity* measures

$$TQ_1 := \mu_{4/3}^{-3}\frac{n^2}{(n-2)T}\sum_{i=2}^{n-1}|\delta_i(p)|^{4/3}|\delta_{i-1}(p)|^{4/3}|\delta_{i-2}(p)|^{4/3}, \tag{18}$$

$$TQ_2 := \mu_{4/3}^{-3} \frac{n}{T} \sum_{i=2}^{n-1} |\delta_i(p)|^{4/3} |\delta_{i-1}(p)|^{4/3} |\delta_{i-2}(p)|^{4/3},$$

where $\mu_p = E(|Z|^p)$ and Z denotes a standard normally distributed random variable. These estimators are consistent in the absence of microstructure noise and robust to jumps and hence they allow for the construction of feasible tests for the presence of jumps. Motivated by the desire for robustness against i.i.d. noise, a staggered version of the tripower quarticity measure (18) is defined by [Andersen et al., 2006]

$$TQ^{(k)} := \mu_{4/3}^{-3} \frac{n^2}{(n-2-2k)T} \sum_{i=2+2k}^{n-1} |\delta_i(p)|^{4/3} |\delta_{i-(1+k)}(p)|^{4/3} |\delta_{i-2(1+k)}(p)|^{4/3},$$

where k is any positive but finite integer. However, in practice, if k is large then the staggered estimator is likely to have a large finite sample bias.

A further generalization is given by multipower variation measures, such as the *realized quadpower quarticity* proposed by [Barndorff-Nielsen and Shephard, 2006]

$$QQ := \mu_1^{-4} \frac{n}{T} \sum_{i=3}^{n-1} |\delta_i(p)||\delta_{i-1}(p)||\delta_{i-2}(p)||\delta_{i-3}(p)|.$$

Recently, [Jacod et al., 2009] proposed a pre-averaging technique as an alternative to subsampling in order to reduce the microstructure effects. The idea is that if one averages a number of observed log-prices, one is closer to the latent process $p(t)$. This approach, when well implemented, gives rise to rate optimal estimators of power variations. In particular, a consistent estimator of the integrated quarticity can be constructed as

$$Q_{av} = \frac{1}{3\theta^2\psi_2^2} \sum_{i=0}^{n-k_n+1} (\bar{p}_i^n)^4 - \frac{\rho(n)\psi_1}{\theta^4\psi_2^2} \sum_{i=0}^{n-2k_n+1} (\bar{p}_i^n)^2 \sum_{j=i+k_n}^{i+2k_n-1} (\delta_j(p))^2 + \frac{\rho(n)\psi_1^2}{4\theta^4\psi_2^2} \sum_{i=0}^{n-3} (\delta_i(p))^2 (\delta_{i+2}(p))^2,$$

where the pre-averaged price process is given by

$$\bar{p}_i^n = \frac{1}{k_n} \left(\sum_{j=k_n/2}^{k_n-1} p_{i+j} - \sum_{j=0}^{k_n/2-1} p_{i+j} \right),$$

$\theta = k_n \sqrt{\rho(n)}$, $\psi_1 = 1$ and $\psi_2 = 1/12$, corresponding to a "hat" weight function, and k_n is a suitable integer.

Finally, our analysis is not extended to the Nearest Neighbor Truncation estimators recently proposed by [Andersen et al., 2011] because these estimators are specifically designed to cope with jumps but are less efficient than the multipower variation statistics in scenarios without jumps.

We simulate second-by-second return and variance paths over a daily trading period of $T = 6$ hours, for a total of 252 trading days and $n = 21600$ observation per day. The infinitesimal variation of the true log-price process and spot volatility is given by the CIR square-root model [Cox et al., 1985]

$$\begin{aligned} dp(t) &= \sigma(t)\ dW_1(t) \\ d\sigma^2(t) &= \alpha(\beta - \sigma^2(t))dt + \nu\sigma(t)\ dW_2(t), \end{aligned} \tag{19}$$

where W_1, W_2 are independent Brownian motions. The parameter values used in the simulations are taken from the unpublished Appendix to [Bandi and Russell, 2005] and reflect the features of IBM time series: $\alpha = 0.01$, $\beta = 1.0$, $\nu = 0.05$. The initial value of σ^2 is set equal to one, while $p(0) = \log 100$. Moreover, when microstructure effects are considered, we assume that the logarithmic noises η are Gaussian i.i.d. and independent from p; this is typical of bid-ask bounce effects in the case of exchange rates and, to a lesser extent, in the case of equities. We consider a noise-to-signal ratio of $\zeta = 2$ or $\zeta = 4$.

The sampling frequency and the other parameters contained in the definition of the estimators above must be chosen conveniently, especially in the presence of noise. One possible criterion is the minimization of the true MSE. Another possible choice is the minimization of the expected asymptotic error variance. However, both these procedures are unfeasible when applied to empirical data, where the actual volatility path is not observed. Feasible finite sample MSE-based optimal rules for choosing the sampling frequency and the number of subgrids S for subsampling are discussed in [Bandi and Russell, 2006] and [Zhang et al., 2005] with regards to the corresponding integrated variance estimators, while a specific study of optimally designed quarticity estimators in the presence of microstructure effects is still lacking. Hence, for each quarticity estimator, our choice is to employ the optimal sampling frequency and other parameter values implied by the rules of thumb available for the corresponding integrated volatility estimators. This entails the choice $n^* = (T\int_0^T \sigma_t^4 dt/(4(E[\eta^2])^2))^{1/3}$ for any power and multipower quarticity-type estimator and the optimal value $S = n/\bar{n}^*$, with $\bar{n}^* = (T\int_0^T \sigma_t^4 dt/(6(E[\eta^2])^2))^{1/3}$ for the subsampled power and bipower quarticity. Preliminary estimates of the population moment $E[\eta^2]$ can be obtained from quote-to-quote return data according to [Bandi and Russell, 2005], while $\int_0^T \sigma_t^4 dt$ can be preliminarily estimated by computing $Q = n/(3T)\sum_{j=1}^n (\delta_j(\tilde{p}))^4$ using 2-minute returns. In the case of the Pre-averaging estimator, we apply the optimal mean square error bandwidth selection suggested by [Barndorff-Nielsen et al., 2008b] and choose $k_n = c^* \xi^{4/5} n^{3/5}$, where $c^* = (144/0.269)^{1/5}$, $\xi^2 = E[\eta^2]/\sqrt{Q}$ and Q is the integrated quarticity estimated by means of 2-minute returns. We stress the fact that these criteria may be suboptimal with respect to the optimal design of quarticity estimators.

In the case of the Fourier estimator, the theoretical results provided in the previous sections highlight the importance of the cutting parameters N and M. Indeed, the definition of the Fourier estimator of quarticity requires that the econometrician make a choice regarding the highest frequency coefficients $c_k(dp_n)$ and $c_s(\sigma^2_{n,N})$ to be included in the expansion (7). The results in Theorems 3.3 and 4.1 provide asymptotic growth conditions on the parameters N, M and n required to build efficient estimators. However, given n, operatively the optimal parameter values N, M can be easily obtained by direct minimization of the true MSE or, conversely, of an estimate or upper bound of the true MSE. Contrary to the minimization of the true MSE, the second procedure is feasible, in the sense that it relies only on measurable quantities. Therefore, in the absence of microstructure effects a feasible procedure for optimizing the Fourier estimator consists explicitly in minimizing with respect to N, M the upper bound of the MSE provided by Corollary 3.4. In the presence of noise, we can provide only a suboptimal strategy for the choice of N and M since Theorem 4.1 quantifies the difference between the noise affected quarticity estimator and the consistent one $\sigma^4_{n,N,M}$. From a practical point of view, after correcting for the bias due to noise effects as in (14), efficient Fourier estimators having small MSE can be obtained by minimizing a linear combination of the upper bound for the MSE given in Corollary 3.4 and of $\Lambda^2_{n,N,M}(\sigma,\eta)$ with respect to M and N. Hence, for the Fourier methodology we choose

to minimize the functional

$$2\Theta^2_{n,N,M}(\sigma) + 2\Lambda^2_{n,N,M}(\sigma,\eta), \tag{20}$$

where

$$\Theta^2_{n,N,M}(\sigma) := (4\pi)^2\frac{2}{3}M^2 \text{ess sup}\,\|\sigma^2\|^4_{L^\infty}\left((C_1)^{\frac{1}{2}}\rho(n)^2[N^2+M^2] + (C_2)^{\frac{1}{2}}\frac{1}{2N+1}\right)$$

$$+(2\pi)^2\,\text{ess sup}\,\|\sigma^2\|^2_{L^\infty}(\omega_{\sigma^2}(\frac{4}{M}))^2$$

and $\Lambda^2_{n,N,M}(\sigma,\eta)$ is given in (13). Usually, the optimal N turns out to be much smaller than the Nyquist frequency (i.e. $N \ll n/2$) both in the absence and in the presence of noise. Moreover, in complete agreement with the theory developed in Sections 3 and 4, the optimal M is very small.

Taking into account the considerations above, it is important to analyze the sensitivity of the estimator to this choice, with particular regard to the uncorrected version. In Figure 1, we plot the real MSE of $\tilde{\sigma}^4_{n,N,M}$ averaged over the 252 days as a function of M and N, respectively, and of any combination (M,N) both in the presence and in the absence of microstructure effects. We notice that the Fourier estimators turns out to be on average quite robust to the choice of M. As regards to N, except for the lowest values up to about $N = 100$ and depending on M, the MSE exhibits small variability as well but on a larger scale. Thus, N turns out to be the most critical parameter in the design of the Fourier estimator, especially in the presence of noise. The motivation is twofold: (i) the choice of N is crucial for an efficient computation of the coefficients $c_s(\sigma^2_{n,N})$, which are the bricks used to build the quarticity estimate; (ii) the role of M is attenuated by the smoothing Fejer kernel in (7). Hence, most of the microstructure is filtered out by truncating the volatility coefficients (5) up to N, thus neglecting the noisy highest frequency return coefficients.

Nevertheless, we want to stress the different behavior of the MSE in the absence or in the presence of noise. In the absence of noise (left column), the MSE is almost unaffected by the choice of M and seems to be decreasing with respect to N, at least in the range plotted in the picture. Notice that, as predicted by the theory, in the absence of noise the MSE tends to zero as $n, M, N \to \infty$ such that $MN/n, M^2/N \to 0$. On the contrary, when microstructure effects are taken into account, stronger growth conditions on M and N must be fulfilled, namely $MN^2/n, M^3/N \to 0$. Indeed, on the second column of the figure we can see that the MSE of the non corrected Fourier estimator $\tilde{\sigma}^4_{n,N,M}$ tends to increase for large values of M and N, the minimum of the MSE surface being attained at $M = 1$, $N = 250$. Hence the need for the noise correction (14) to further reduce the growth of the MSE with respect to M and for an accurate choice of N to filter out the microstructure effects.

In Figure 2, we show the effect of the noise correction (14) on the real MSE and BIAS. We notice that, as expected, the main scope of this correction is to reduce the growing rate of both MSE and BIAS with respect to M, by subtracting an estimate of the term (11). This is clear from the figure, where we see that the most evident effect of correction is the reduction of the variability of MSE and BIAS with respect to M. This is very important, because the correction makes the Fourier estimator less sensitive to the choice of M in the presence of noise, so that N becomes the crucial parameter in the estimator design.

In Tables 1-5, we provide a comparative analysis of the efficiency of the different estimators of quarticity for the model (19). All the estimators have been optimized as described above, on average over the 252 days. The label "Unfeasible" stands for the non feasible minimization of the

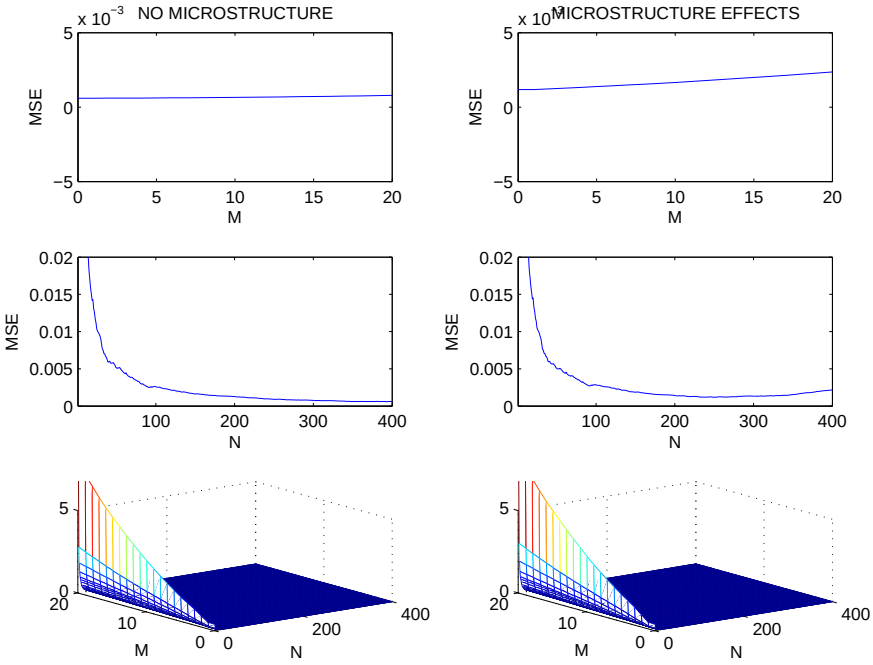

Figure 1: Real MSE of $\tilde{\sigma}^4_{n,N,M}$ averaged over the whole dataset (252 days) as a function of M and N, for the purely diffusive price process (19) and in the presence of microstructure effects, with $\zeta = 4$.

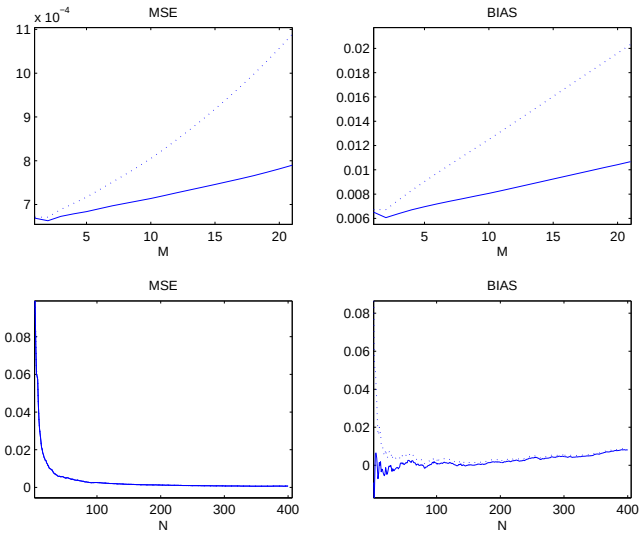

Figure 2: Effect of the noise correction on the real MSE and BIAS of $\tilde{\sigma}^4_{n,N,M}$. The dotted line refers to $\tilde{\sigma}^4_{n,N,M}$, while the solid line refers to the corrected estimator $\hat{\sigma}^4_{n,N,M}$. Noise-to-signal ratio $\zeta = 2$.

	Unfeasible		Feasible	
	MSE	BIAS	MSE	BIAS
$\sigma^4_{n,N,M}$	5.95e-4	1.42e-4	6.18e-4	1.80e-3
RQ	7.11e-5	3.96e-4	7.90e-4	-7.11e-4
BQ	7.88e-5	7.35e-4	8.12e-4	-1.91e-3
Q	9.83e-5	2.27e-4	1.19e-3	-1.09e-4
TQ_1	8.51e-5	2.81e-5	9.51e-4	-1.94e-3
TQ_2	8.51e-5	1.70e-5	9.49e-4	-2.57e-3
$TQ^{(k)}$	9.40e-5	-3.12e-4	1.06e-3	-1.76e-3
QQ	9.54e-5	1.02e-4	1.07e-3	-2.60e-3
RQ_{sub}	4.95e-5	5.18e-4	4.84e-4	-1.20e-3
BQ_{sub}	7.24e-4	-1.36e-2	8.15e-4	-1.88e-2
Q_{av}	2.97e-4	-7.54e-3	3.22e-4	-1.12e-2

Table 1: No noise. "Unfeasible" stands for the "non feasible minimization of the real MSE" over the whole dataset. "Feasible" stands for "feasible MSE-based optimization", based on the minimization of the functional (20) for the Fourier estimator and on the rules of thumb provided by the literature for the other estimators.

real MSE, while "Feasible" refers to the suboptimal feasible procedures of MSE minimization summarized above and based on the minimization of the functional (20) for the Fourier estimator and on the rules of thumb provided by the literature for the other estimators and described above.

Table 1 refers to the ideal case of a purely diffusive price process, with uniformly distributed observations. In this case, the realized quarticity-type estimators RQ, BQ, Q, TQ_1, TQ_2, $TQ^{(k)}$ and QQ perform best when data are sampled at the highest frequency (second-by-second). Hence, in this case all the unfeasible estimators are confronted over the same dataset, at the highest frequency. However, the feasible selection of the sampling interval for the realized quarticity-type estimators provides a frequency of 0.47 min, which is suboptimal. The best estimate is given by RQ_{sub}, where the number of subgrids S selected by the unfeasible minimization is 2. These results make sense, because under the Itô paradigm there is no need for subsampling or pre-averaging. The Fourier estimator $\sigma^4_{n,N,M}$ is in line with these last estimators, but less biased.

One of the most attractive features of the Fourier methodology is its ability to cope with microstructure effects. In fact, a convenient choice of the cutting frequencies M and N makes the Fourier estimator invariant to high frequency noise. In Table 2, we introduce Gaussian i.i.d. microstructure effects of medium intensity ($\zeta = 2$). Both the feasible and unfeasible procedures provide an efficient Fourier estimator $\tilde{\sigma}^4_{n,N,M}$ and corrected version $\hat{\sigma}^4_{n,N,M}$. Only the pre-averaging estimator Q_{av} performs better, thus confirming the ability of the Fourier approach to filter out microstructure effects. The optimal parameter values selected by the unfeasible procedure are $N = 357$, $M = 2$, while the values selected by the feasible procedure are $N = 350$, $M = 3$. The optimal unfeasible sampling interval for the realized quarticity-type estimators ranges from 1.55 to 2.19 min, while the optimal interval provided by the rule-of-thumb is 1.94 min. Therefore, we stress the fact that, unlike for $\tilde{\sigma}^4_{n,N,M}$, $\hat{\sigma}^4_{n,N,M}$,RQ_{sub}, BQ_{sub} and Q_{av}, the realized quarticity-type estimators work on subsets of available data, using sparse sampling to reduce microstructure effects.

In Table 3, the noise-to-signal ratio is raised to $\zeta = 4$. In this case, the realized quarticity-

	Unfeasible		Feasible	
	MSE	BIAS	MSE	BIAS
$\tilde{\sigma}^4_{n,N,M}$	6.71e-4	6.72e-3	7.21e-4	8.09e-3
$\hat{\sigma}^4_{n,N,M}$	6.65e-4	6.27e-3	7.01e-4	6.75e-3
RQ	4.48e-3	4.08e-2	5.44e-3	3.18e-2
BQ	4.71e-3	2.29e-2	5.67e-3	3.01e-2
Q	5.46e-3	3.96e-2	7.45e-3	3.26e-2
TQ_1	5.45e-3	2.36e-2	7.34e-3	3.75e-2
TQ_2	5.19e-3	2.03e-2	6.99e-3	3.44e-2
$TQ^{(k)}$	5.89e-3	3.89e-2	8.41e-3	3.90e-2
QQ	5.38e-3	2.07e-2	7.21e-3	3.34e-2
RQ_{sub}	3.16e-3	2.90e-2	3.17e-3	2.78e-2
BQ_{sub}	7.59e-4	-1.43e-2	2.41e-3	-9.56e-3
Q_{av}	3.39e-4	-6.81e-3	4.36e-4	-3.37e-3

Table 2: Microstructure effects ($\zeta = 2$). Same format as Table 1.

	Unfeasible		Feasible	
	MSE	BIAS	MSE	BIAS
$\tilde{\sigma}^4_{n,N,M}$	1.18e-3	1.62e-2	1.31e-3	1.71e-2
$\hat{\sigma}^4_{n,N,M}$	7.43e-4	1.14e-4	1.03e-3	-9.57e-4
RQ	1.05e-2	1.11e-2	1.38e-2	5.79e-2
BQ	1.21e-2	3.17e-2	1.68e-2	6.05e-2
Q	1.36e-2	3.23e-2	1.74e-2	5.66e-2
TQ_1	1.49e-2	3.14e-2	2.07e-2	6.77e-2
TQ_2	1.35e-2	2.25e-2	1.91e-2	6.04e-2
$TQ^{(k)}$	1.36e-2	3.81e-2	1.90e-2	6.64e-2
QQ	1.37e-2	1.52e-2	1.87e-2	5.51e-2
RQ_{sub}	7.08e-3	3.35e-2	7.35e-3	4.80e-2
BQ_{sub}	8.37e-4	-1.55e-2	4.96e-3	-1.48e-2
Q_{av}	5.05e-4	-3.59e-3	7.55e-4	-1.83e-3

Table 3: Microstructure effects ($\zeta = 4$). Same format as Table 1.

	Unfeasible		Feasible	
	MSE	BIAS	MSE	BIAS
$\sigma^4_{n,N,M}$	6.62e-4	-2.60e-3	7.01e-4	3.52e-4
RQ	1.06e-3	9.03e-3	2.52e-3	-2.21e-3
BQ	8.69e-4	-1.25e-2	2.42e-3	-6.19e-3
Q	1.69e-3	5.47e-3	3.80e-3	-2.21e-4
TQ_1	1.12e-3	-1.63e-2	2.72e-3	-6.64e-3
TQ_2	1.13e-3	-1.69e-2	2.71e-3	-8.45e-3
$TQ^{(k)}$	1.02e-3	-1.05e-2	2.66e-3	-2.96e-3
QQ	1.32e-3	-1.94e-2	3.10e-3	-8.47e-3
RQ_{sub}	7.85e-4	1.03e-2	1.86e-3	-4.85e-3
BQ_{sub}	3.31e-3	-3.76e-2	3.81e-3	-4.83e-2
Q_{av}	7.93e-4	-5.95e-3	8.79e-4	-7.67e-3

Table 4: Irregular trading times and no noise. Same format as Table 1.

type estimators provide poor estimates of quarticity and the optimal unfeasible sampling interval ranges from 4.69 to 7.05 min, while the optimal interval provided by the rule-of-thumb is 4.09 min. In this setting of marked noise, the noise correction to the Fourier estimator becomes effective and $\hat{\sigma}^4_{n,N,M}$ becomes the second best estimator after Q_{av} and less biased. The optimal parameter values selected by the unfeasible procedure for $\tilde{\sigma}^4_{n,N,M}$ are $N = 250$, $M = 1$, while the values selected by the feasible procedure are $N = 242$, $M = 3$. Notice, however, that the optimal unfeasible corrected estimator is given by the larger values $N = 343$, $M = 5$. We note that the feasible corrected estimator $\hat{\sigma}^4_{n,N,M}$ is more efficient in terms of both MSE and BIAS than the unfeasible version of $\tilde{\sigma}^4_{n,N,M}$. This means that further coefficients $c_s(\sigma^2_{n,N})$ are actually required in $\hat{\sigma}^4_{n,N,M}$ to provide a more efficient quarticity estimate than simply squaring the integrated variance estimate (see Remark 3.2).

On the whole, we can conclude that both the feasible and unfeasible procedures provide an efficient Fourier estimator. Only the pre-averaging estimator Q_{av} performs better, although it is slightly more biased.

Finally, [Andersen et al., 2011] point out that, unlike volatility estimators, integrated quarticity estimators are badly affected by irregular trading. This occurs because all the considered estimators, except Fourier, assume equal spacing and involve a multiplication by n/T. In order to highlight this issue, we simulate a scenario with Poisson irregular trading times with durations between observations drawn from an exponential distribution with means $\lambda = 5$ sec. See Tables 4 and 5. Indeed, in the scenario of Table 4 the most efficient quarticity estimate is given by $\sigma^4_{n,N,M}$, immediately followed by Q_{av}, both in the unfeasible and in the feasible variant. The remaining estimators are less efficient. Notice that, although no microstructure effects are taken into account, the optimal sampling interval for the realized quarticity-type estimators ranges from 0.4 to 0.69 min.

Finally, in Table 5 we introduce moderate microstructure effects. The corrected Fourier estimator $\hat{\sigma}^4_{n,N,M}$ is indisputably the most efficient estimator, at least in its unfeasible version with the optimal parameter values $N = 354$, $M = 17$. The feasible optimization of the estimator leads to the same efficiency as for Q_{av}, with $N = 327$, $M = 5$. This suboptimality may be caused also by the fact that our feasible MSE minimization procedure assumes uniform distribution of

	Unfeasible		Feasible	
	MSE	BIAS	MSE	BIAS
$\tilde{\sigma}^4_{n,N,M}$	1.79e-3	1.93e-2	4.87e-3	6.14e-2
$\hat{\sigma}^4_{n,N,M}$	9.36e-4	-1.31e-3	2.45e-3	3.72e-2
RQ	4.94e-3	3.96e-2	6.23e-3	3.06e-2
BQ	4.74e-3	3.72e-2	6.12e-3	2.43e-2
Q	6.68e-3	3.95e-2	8.66e-3	3.38e-2
TQ_1	5.42e-3	3.32e-2	7.10e-3	2.72e-2
TQ_2	5.16e-3	3.05e-2	6.75e-3	2.36e-2
$TQ^{(k)}$	5.50e-3	2.69e-2	8.39e-3	2.93e-2
QQ	5.40e-3	2.96e-2	7.24e-3	2.36e-2
RQ_{sub}	3.26e-3	2.41e-2	3.30e-3	2.19e-2
BQ_{sub}	2.88e-3	-2.81e-2	3.32e-3	-2.54e-2
Q_{av}	1.75e-3	1.43e-2	1.92e-3	2.46e-2

Table 5: Irregular trading times and microstructure effects ($\zeta = 2$). Same format as Table 1.

Variable	Mean	Std. Dev.	Min	Max
S&P 500 index futures	893.97	366.24	295.60	1574.00
N. of ticks per minute	7.0433	3.5276	1	56

Table 6: Summary statistics for the sample of the traded CME S&P 500 index futures in the period January 2, 1990 to December 29, 2006 (11,611,297 trades). "Std. Dev." denotes the sample standard deviation of the variable.

trades. Deeper analysis in more general settings is in order.

In conclusion, our discussion shows that the Fourier quarticity estimator is robust to microstructure effects of increasing extent and to non uniform trading data. In particular, cutting the highest frequencies of the observed process makes this estimator almost invariant to the presence of high-frequency noise components.

6.2 An application to S&P 500 index futures

Our empirical application is based on tick-by-tick data of S&P 500 index futures recorded at the Chicago Mercantile Exchange (CME). The sample covers the period from January 2, 1990 to December 29, 2006, a period of 4,274 trading days, having 11,611,297 tick-by-tick observations. Table 6 describes the main features of our data set.

High frequency returns are contaminated by transaction costs, bid-and-ask bounce effects, etc., leading to biases in the variance measures. Computation of quarticity amplifies both noise and errors, so that data filtering is necessary. Days with trading period shorter than 5 hours have been removed. Jumps have been identified and measured using the Threshold Bipower Variation method (TBV) of [Corsi et al., 2010], which is based on the joint use of bipower variation and threshold estimation [Mancini, 2009]. This method provides a powerful test for jump detection, which is employed at the significance level of 99.9%. This procedure allows to identify a percentage of days with jumps around 27%. Since the TBV estimator is not robust to microstructure noise, we compute the TBV measure of the integrated volatility using 2-minute

returns, which is optimal given the high liquidity of the S&P 500 index futures market. The number of days remaining after jump removal and filtering is 3,078, for a total of 8,575,527 tick-by-tick data. The contribution coming from overnight returns is neglected.

Sparse sampling needed for the realized quarticity-type estimators can be performed either in *calendar time*, which is the most widely used for instance with prices sampled every 5 or 15 minutes, or in *transaction time*, where prices are recorded every m-th transaction. When we sample in calendar time, the x-minute returns are constructed using the nearest neighbor to the x-minute tag. Since trading times are not uniformly distributed along time, quarticity measures are more unstable under transaction time sampling because a given number m of ticks may correspond to quite different time intervals. This non-uniformity of data distribution affects the realized quarticity-type measure, as shown in Figure 3 depicting the average integrated quarticity over the full sample period constructed for different frequencies in calendar (Panel A) and transaction time (Panel B). The quarticity signature plots clearly indicate that the bias induced by market microstructure effects is relatively small for the highly liquid S&P 500 index futures, and dies out very quickly. Note that with a transaction taking place on average about every 8.57 seconds, the average quarticity measure based on 1-minute intervals corresponds to around the 7-th tick presented in the figure, with large variability across the whole dataset. The impact of market microstructure effects on the five-minute realized volatility measure for the S&P 500 index futures over the period from 1990 to 2006 can therefore be regarded as negligible. For sampling frequency lower than 15 min, i.e. for sampling intervals larger than 100 ticks, the different realized quarticity measures start to depart from each other and, when sampled in transaction time, become more variable. We can state that BQ, TQ_1, TQ_2 and QQ remain flat at higher frequencies in calendar time than the other estimators, which are more severely upwards biased at the highest frequencies. On the contrary, for frequencies lower than 15 minutes these same estimators become more downwards biased together with $TQ^{(k)}$.

In Figure 4, we plot the quarticity signature plot, as computed by means of $\hat{\sigma}^4_{n,N,M}$, RQ_{sub}, BQ_{sub} and Q_{av} , using tick-by-tick data as a function of their main parameters N, S, $\tilde{n}$ and k_n respectively. In the Fourier estimator, the value of the parameter M is set to 6, which is the optimal value obtained by our feasible procedure. The sample moments of the noise necessary for the optimization have been computed using quote-to-quote return data, according to $E[\eta^2] = \sum_{i=0}^{n-1} \delta_i(p)^2/(2(n-1))$, $E[\varepsilon^4] = \sum_{i=0}^{n-1} \delta_i(p)^4/n$. The quarticity signature plot is displayed as a function of the other parameter N. In Panel A, we plot both the corrected estimator $\hat{\sigma}^4_{n,N,M}$ (solid line) and the non corrected one $\tilde{\sigma}^4_{n,N,M}$ (dotted line). We can see that for N larger than 100 both estimates become much stable. Taking into account the mathematical properties of the Fourier estimator, when the trading period is $T = 6.5$ hours, a parameter value of say $N = 400$ corresponds to sampling frequencies of $T/(2N) = 390/800 = 0.4875$ min, in the sense that the spectral decomposition in the frequency space allows to detect phenomena happening at the frequency of about half a minute, much higher than with the realized quarticity-type estimators. The remaining estimators provide slightly lower quarticity estimates. Since $\tilde{n}S = n$ in a day, the two parameters $\tilde{n}$ and S play an opposite role. In particular, the interval $50 \leq \tilde{n} \leq 60$ roughly corresponds to the interval $20 \leq S \leq 30$. Moreover, Q_{av} seems to be quite stable for $k_n \geq 20$. Finally, by comparing results in Figure 4 with those in Figure 3, we notice that the realized quarticity-type estimates are slightly upper biased.

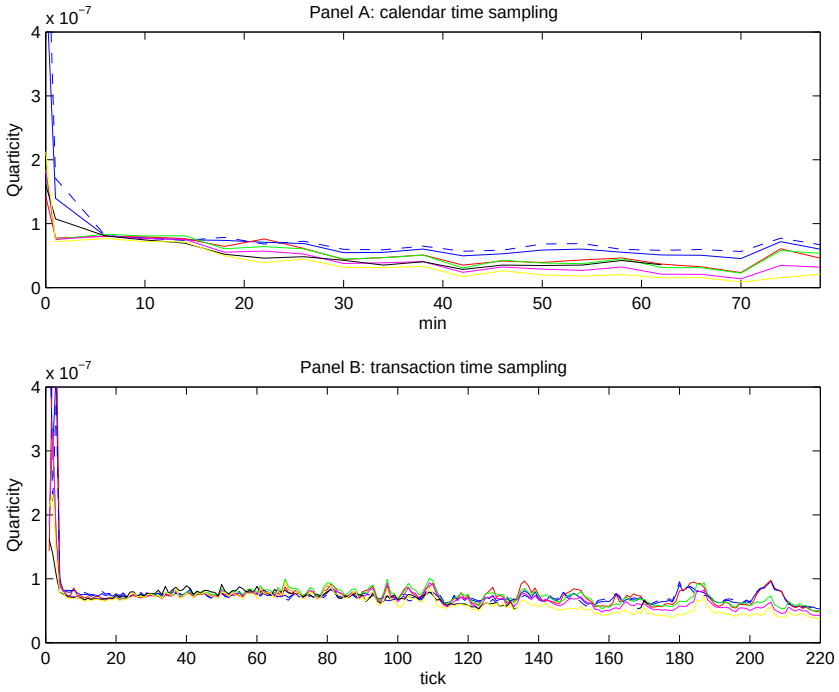

Figure 3: Quarticity signature plot of the S&P 500 index futures constructed over the full sample period. The graph shows average integrated quarticity constructed for different frequencies measured minutes (Panel A) and in number of ticks (Panel B). Note that there are about 8.57 seconds on average between trades, so that the average annualized 5-minute based realized volatility corresponds to around the 35th tick. RQ solid blue line; BQ red line; Q dashed blue line; TQ_1 green line; TQ_2 magenta line; $TQ^{(k)}$ black line; QQ yellow line.

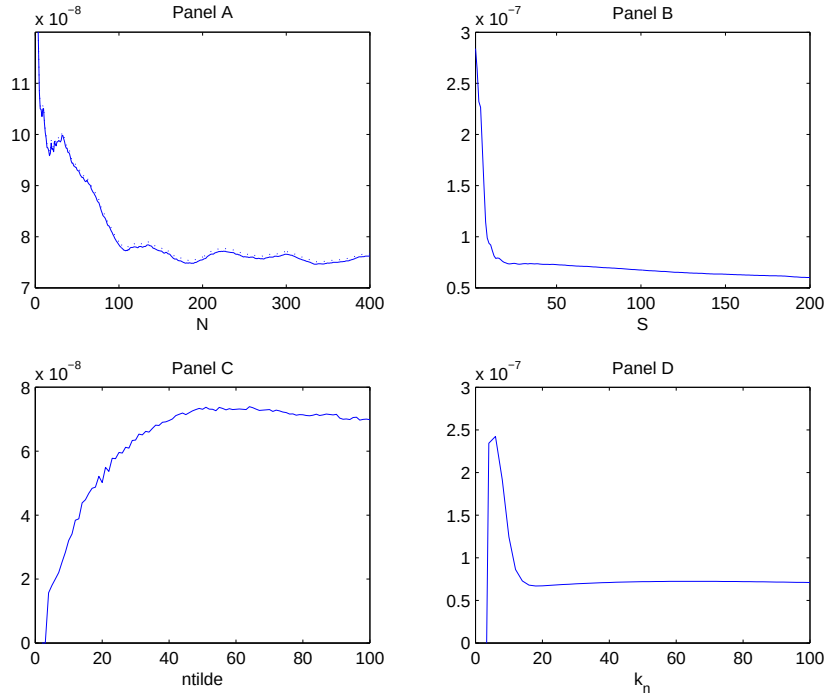

Figure 4: Quarticity signature plot of the S&P 500 index futures constructed over the full sample period. The graph shows average integrated quarticity computed by means of $\hat{\sigma}^4_{n,N,M}$, RQ_{sub}, BQ_{sub} and Q_{av} , using tick-by-tick data, as a function of their main parameters.

7 Conclusions

We propose a new methodology based on Fourier analysis to estimate the fourth power of volatility function (spot quarticity) and, in particular, the integrated quarticity. The Fourier methodology allows to reconstruct the latent instantaneous volatility as a series expansion with coefficients gathered from the Fourier coefficients of the observable price variation and can be easily extended to higher even powers of volatility and to the multivariate case.

We prove that the Fourier estimator of integrated quarticity is consistent in the absence of noise. Moreover, we propose a corrected version which is more efficient in the presence of microstructure effects. The efficiency of the Fourier estimator largely depends on the choice of two parameters M and N, which define the highest frequency Fourier coefficients taken into account by the estimator. This choice is partly related to the extent of the microstructure effects present in the data. Therefore, we address the problem of constructing an optimal MSE-based Fourier quarticity estimator, which renders our methodology feasible with real data on finite samples.

The new methodology is tested in realistic Monte Carlo experiments and in an empirical application to S&P 500 index futures. We make a comparative analysis of the performance of most of the estimators existing in the literature. Our analysis shows that a very attractive feature of the Fourier methodology is its ability to cope with microstructure effects and with non uniformity of trading data.

References

[Andersen and Bollerslev, 1998] Andersen, T. and Bollerslev, T. (1998) Answering the skeptics: yes, standard volatility models do provide accurate forecasts. *International Economic Review*, 39/4, 885–905.

[Andersen and al., 1999] Andersen, T., Bollerslev, T., Diebold, F. and Labys, P. 1999. (Understanding, optimizing, using and forecasting) Realized volatility and correlation. *New York Univ., Stern School Finance Dept. Working paper*, 99-061.

[Andersen et al., 2001] Andersen, T., Bollerslev, T., Diebold, F. and Ebens, H. (2001). The distribution of realized stock return volatility. *Journal of Financial Economics*, 61, 43–76.

[Andersen et al., 2006] Andersen, T.G., Bollerslev, T., Frederiksen, P.H., and Nielsen, M.Ø. (2006) Comment on P. R. Hansen and A. Lunde: Realized variance and market microstructure noise. *Journal of Business and Economic Statistics*, 24, 173-179.

[Andersen et al., 2011] Andersen, T., Dobrev, D. and Schaumburg, E. (2011). A Functional filtering and neighborhood truncation approach to integrated quarticity estimation. *Working Paper*.

[Bandi and Russell, 2005] Bandi, F.M. and Russell, J.R. (2005). Microstructure noise, realized variance and optimal sampling. *Working paper, Univ. of Chicago* http://faculty.chicagogsb.edu/federicobandi.

[Bandi and Russell, 2006] Bandi, F.M. and Russell, J.R. (2006). Market microstructure noise, integrated variance estimators, and the accuracy of asymptotic approximations. *Working paper, Univ. of Chicago* http://faculty.chicagogsb.edu/federicobandi.

[Barndorff-Nielsen et al., 2006] Barndorff-Nielsen, O.E., Graversen, S.E., Jacod, J. and Shephard, N. (2006). Limit theorems for realised bipower variation in econometrics. *Econometric Theory*, 22.

[Barndorff-Nielsen et al., 2008a] Barndorff-Nielsen, O.E., Hansen, P.R., Lunde, A. and Shephard, N. (2008). Designing realised kernels to measure the ex-post variation of equity prices in the presence of noise. *Econometrica*, 76/6, 1481–1536.

[Barndorff-Nielsen et al., 2008b] Barndorff-Nielsen, O.E., Hansen, P.R., Lunde, A. and Shephard, N. (2008) Multivariate Realised kernels: consistent positive semi-definite estimators of the covariation of equity prices with noise and non-synchronous trading. *Working paper*.

[Barndorff-Nielsen and Shephard, 2002] Barndorff-Nielsen, O.E. and Shephard, N. (2002) Econometric analysis of realized volatility and its use in estimating stochastic volatility models. *Journal of the Royal Statistical Society*, Series B, 64, 253–280.

[Barndorff-Nielsen and Shephard, 2004a] Barndorff-Nielsen, O.E., and Shephard, N. 2004. Power and bipower variation with stochastic volatility and jumps (with discussion). *Journal of Financial Econometrics*, 2, 1–48.

[Barndorff-Nielsen and Shephard, 2004b] Barndorff-Nielsen, O.E. and Shephard, N. (2004) Econometric analysis of realized covariation: high frequency based covariance, regression and correlation in financial economics. *Econometrica*, 72/3, 885–925.

[Barndorff-Nielsen and Shephard, 2006] Barndorff-Nielsen, O.E. and Shephard, N. (2006) Econometrics of testing for jumps in financial economics using bipower variation. *Journal of Financial Econometrics*, 4, 1–30.

[Corsi et al., 2010] Corsi, F., Pirino, D. and Renó, R. (2010) Threshold bipower variation and the impact of jumps on volatility forcasting. *Journal of Econometrics*, 159 (2), 276-288.

[Cox et al., 1985] Cox, J.C., Ingersoll, J.E. and Ross, S.A. (1985). A theory of the term structure of interest rates. *Econometrica*, 53, 385–408.

[Ghysels and Sinko, 2007] Ghysels, E. and Sinko, A. (2007). *Volatility forecasting and microstructure noise*, Working Paper.

[Gatheral and Oomen, 2010] Gatheral, and Oomen, R.C.A. (2010) Zero intelligence realized variance estimation. *Finance and Stochastics*, 14 (2), 249–283.

[Hayashi and Yoshida, 2005] Hayashi, T. and Yoshida, N. (2005) On covariance estimation of nonsynchronously observed diffusion processes. *Bernoulli*, 11 (2), 359–379.

[Hansen and Lunde, 2006] Hansen, P.R. and Lunde, A. 2006. Realized variance and market microstructure noise (with discussions). *Journal of Business and Economic Statistics*, 24, 127–218.

[Jacod et al., 2009] Jacod, J., Li. Y., Mykland, P.A., Podolskij, M. and Vetter, M. (2009). Microstructure noise in the continuous case: the pre-averaging approach. *Stochastic Processes and their Applications*, 119, 2249-2276.

[Jiang and Oomen, 2008] Jiang, G.J. and Oomen, R.C. 2008. Testing for jumps when asset prices are observed with noise - a "swap variance" approach. *Journal of Econometrics*, 144 (2), 352-370.

[Lo and MacKinlay, 1990] Lo, A. and MacKinlay, C. (1990) The econometric analysis of nonsynchronous trading. *Journal of Econometrics*, 45, 181–211.

[Malliavin, 1995] Malliavin, P. (1995). *Integration and Probability*, Springer Verlag.

[Malliavin and Mancino, 2002] Malliavin, P. and Mancino, M.E. (2002). Fourier series method for measurement of multivariate volatilities. *Finance and Stochastics*, 4, 49–61.

[Malliavin and Mancino, 2009] Malliavin, P. and Mancino, M.E. (2009). A Fourier transform method for nonparametric estimation of multivariate volatility. *Annals of Statistics,* 37 (4), 1983–2010.

[Mancini, 2009] Mancini, C. (2009) Non-parametric threshold estimation for models with stochastic diffusion coefficient and jumps. *Scandinavian Journal of Statistics*, 36, 270–296.

[Mancino and Sanfelici, 2008] Mancino, M.E. and Sanfelici, S. (2008) Robustness of Fourier Estimator of Integrated Volatility in the Presence of Microstructure Noise. *Computational Statistics and Data Analysis*, 52(6), 2966–2989.

[Mancino and Sanfelici, 2010] Mancino, M.E. and Sanfelici, S. (2010) Estimating covariance via Fourier method in the presence of asynchronous trading and microstructure noise. *Journal of Financial Econometrics* .

[Mykland, 2007] Mykland, P.A. (2007). A Gaussian calculus for inference from high frequency data. *Working Paper, University of Chicago.*

[Podolskij and Vetter, 2009] Podolskij, M. and Vetter, M. (2009) Estimation of Volatility Functionals in the Simultaneous Presence of Microstructure Noise and Jumps. *Bernoulli*, 15, 634–658.

[Renó, 2003] Renó, R. (2003) A closer look at the Epps effect. *International Journal of Theoretical and Applied Finance*, 6 (1), 87–102.

[Roll, 1984] Roll, R. (1984). A simple measure of the bid-ask spread in an efficient market. *Journal of Finance*, 39, 1127–1139.

[Schulz, 2010] Schulz, F.C. (2010). Robust estimation of integrated variance and quarticity under flat price and no trading bias. *Working Paper.*

[Zamansky, 1949] Zamansky, M. (1949) Classes de saturation de certains procédés d'approximation des séries de Fourier des fonctions continues et applications à quelques problèmes d'approximation. *Annales scientifiques de l'É.N.S.* 3^e série, t.66: 19-93.

[Zhang, 2006] Zhang, L. (2006) Estimating Covariation: Epps Effect, Microstructure Noise. *Working paper.*

[Zhang et al., 2005] Zhang, L., Mykland, P. and Aït-Sahalia, Y. (2005). A tale of two time scales: determining integrated volatility with noisy high frequency data. *Journal of the American Statistical Association,* 100, 1394–1411.

[Zhou, 1996] Zhou, B. 1996. High frequency data and volatility in foreign-exchange rates. *Journal of Business and Economic Statistics*, 14(1), 45–52.

8 Appendix: Proofs

For simplicity in the proofs we will write $c_k(\sigma^2) := \mathcal{F}(\sigma^2)(k)$.

Proof. of Proposition 2.2.
Denote $\sigma^2_M(t) := \sum_{|k|\leq M} e^{\mathrm{i}kt} c_k(\sigma^2)$. Consider the square integrable process $\sigma^4(t)$, by assumption **(A.I)**. By orthogonality argument it holds:

$$c_n(\sigma^4_M) = \sum_{|k|\leq M} c_{n-k}(\sigma^2)c_k(\sigma^2).$$

Then as σ^4_M converges to σ^4 in L^2-norm, it follows that $\lim_M \sum_{|k|\leq M} c_{n-k}(\sigma^2)c_k(\sigma^2) = c_n(\sigma^4)$ in probability. □

In order to prove Theorem 3.3 we show two preliminary Lemmas.

Lemma 8.1 *For any $|s| \leq M$ it holds*

$$E[|\frac{2\pi}{2N+1} \sum_{|k|\leq N} c_k(dp_n)c_{s-k}(dp_n) - c_k(dp)c_{s-k}(dp)|^4] \leq C_1 \operatorname{ess\,sup} \|\sigma^2\|^4_{L^\infty} \rho(n)^4 (N^4 + (N+M)^4), \tag{21}$$

where $C_1 = 2^6 \cdot 7$.

Proof. of Lemma 8.1
For any $|k| \leq N$ we have:

$$E[|c_k(dp_n)c_{s-k}(dp_n) - c_k(dp)c_{s-k}(dp)|^4] \leq$$

$$\leq 2^3 \left\{ E[|c_k(dp)|^8]^{\frac{1}{2}} E[|c_{k-s}(dp_n) - c_{k-s}(dp_n)|^8]^{\frac{1}{2}} + E[|c_{k-s}(dp_n)|^8]^{\frac{1}{2}} E[|c_k(dp_n) - c_k(dp_n)|^8]^{\frac{1}{2}} \right\}.$$

By Burkholder-Davis-Gundy inequality, for any $|k| \leq N$

$$E[|c_k(dp_n) - c_k(dp_n)|^8] \leq \frac{56}{(2\pi)^4} \operatorname{ess\,sup} \|\sigma^2\|_{L^\infty}^4 k^8 \rho(n)^8.$$

Thus

$$E[|c_k(dp_n)c_{s-k}(dp_n) - c_k(dp)c_{s-k}(dp)|^4] \leq 2^3 \frac{56}{(2\pi)^4} \operatorname{ess\,sup} \|\sigma^2\|_{L^\infty}^4 \rho(n)^4 (N^4 + (N+M)^4).$$

Then (21) follows. □

Lemma 8.2 *For any $|s| \leq M$ it holds*

$$E[|\frac{2\pi}{2N+1} \sum_{|k| \leq N} c_k(dp)c_{s-k}(dp) - c_s(\sigma^2)|^4] \leq C_2 \operatorname{ess\,sup} \|\sigma^2\|_{L^\infty}^4 \frac{1}{(2N+1)^2}, \tag{22}$$

where $C_2 = 9 \cdot \frac{2^7}{\pi}$.

Proof. of Lemma 8.2
By Itô formula:

$$E[|\frac{2\pi}{2N+1} \sum_{|k| \leq N} c_k(dp)c_{s-k}(dp) - c_s(\sigma^2)|^4] = \frac{1}{\pi^4} E[|\int_0^{2\pi} dp(u) A_N(u)|^4]$$

where

$$A_N(u) := \int_0^u e^{\mathrm{i}kv} D_N(u-v) dp(v).$$

By Burkholder-Davis-Gundy inequality and Holder inequality we have

$$E[|\int_0^{2\pi} dp(u) A_N(u)|^4] \leq 12 \cdot 2\pi \operatorname{ess\,sup} \|\sigma^2\|_{L^\infty}^2 E[\int_0^{2\pi} A_N^4(t) dt]$$

$$\leq (12)^2 (2\pi)^3 \operatorname{ess\,sup} \|\sigma^2\|_{L^\infty}^4 (\frac{1}{2N+1})^2.$$

□

Proof. of Theorem 3.3

$$E[|\sigma_{n,N,M}^4 - \int_0^{2\pi} \sigma^4(t) dt|^2]$$

$$\leq 2 \left\{ E[|2\pi \sum_{|s|<M} (1 - \frac{|s|}{M}) \{c_s(\sigma_{n,N}^2) c_{-s}(\sigma_{n,N}^2) - c_s(\sigma^2) c_{-s}(\sigma^2)\}|^2] \right. \tag{23}$$

$$+ E[|2\pi \sum_{|s|<M} (1 - \frac{|s|}{M}) c_s(\sigma^2) c_{-s}(\sigma^2) - \int_0^{2\pi} \sigma^4(t) dt|^2] \Bigg\}. \quad (24)$$

Consider (23). For any $|s| < M$ it holds

$$E[|c_s(\sigma^2_{n,N}) c_{-s}(\sigma^2_{n,N}) - c_s(\sigma^2) c_{-s}(\sigma^2)|^2]$$

$$\leq 2\{E[|c_s(\sigma^2_{n,N})|^4]^{\frac{1}{2}} E[|c_{-s}(\sigma^2_{n,N}) - c_{-s}(\sigma^2)|^4]^{\frac{1}{2}} + E[|c_{-s}(\sigma^2)|^4]^{\frac{1}{2}} E[|c_s(\sigma^2_{n,N}) - c_s(\sigma^2)|^4]^{\frac{1}{2}}\}.$$

By Minkowski inequality and applying Lemma 8.1 and Lemma 8.2:

$$E[|c_s(\sigma^2_{n,N}) - c_s(\sigma^2)|^4]^{\frac{1}{2}} \leq$$

$$\leq 2(C_1)^{\frac{1}{2}} \operatorname{ess\,sup} \|\sigma^2\|^2_{L^\infty} \rho(n)^2 (N^4 + (N+M)^4)^{\frac{1}{2}} + 2(C_2)^{\frac{1}{2}} \operatorname{ess\,sup} \|\sigma^2\|^2_{L^\infty} \frac{1}{2N+1}.$$

Therefore for any $|s| < M$ it holds

$$E[|c_s(\sigma^2_{n,N}) c_{-s}(\sigma^2_{n,N}) - c_s(\sigma^2) c_{-s}(\sigma^2)|^2] \leq$$

$$\leq 2^2 \operatorname{ess\,sup} \|\sigma^2\|^4_{L^\infty} \left((C_1)^{\frac{1}{2}} \rho(n)^2 (N^4 + (N+M)^4)^{\frac{1}{2}} + (C_2)^{\frac{1}{2}} \frac{1}{2N+1} \right).$$

Finally (23) is less than

$$(4\pi)^2 M \sum_{|s|<M} (1 - \frac{|s|}{M})^2 \operatorname{ess\,sup} \|\sigma^2\|^4_{L^\infty} \left((C_1)^{\frac{1}{2}} \rho(n)^2 [N^2 + (N+M)^2] + (C_2)^{\frac{1}{2}} \frac{1}{2N+1} \right),$$

which goes to 0 under the hypothesis: $\rho(n)NM \to 0$ and $\frac{M^2}{N} \to 0$.

Consider (24). For any $|k| \leq M$, we have

$$E[|2\pi \sum_{|s|<M} (1 - \frac{|s|}{M}) c_s(\sigma^2) c_{-s}(\sigma^2) - \int_0^{2\pi} \sigma^4(t) dt|^2]$$

$$\leq 4\pi \operatorname{ess\,sup} \|\sigma^2\|^2_\infty E[\sup_t |\sigma^2(t) - \sum_{|k|<M} \exp^{\mathrm{i}kt} c_k(\sigma^2)|^2] \leq 4\pi \operatorname{ess\,sup} \|\sigma^2\|^2_\infty (\omega_{\sigma^2}(\frac{4}{M}))^2,$$

where the last inequality follows by [Zamansky, 1949] and we denoted by $\omega_{\sigma^2}(\lambda)$ the modulus of continuity of the variance function. □

Proof. of Corollary 3.4.
It follows by the estimations obtained in the proof in Theorem 3.3. □

Proof. of Theorem 4.1.
We have:

$$\widetilde{\sigma}^4_{n,N,M} - \sigma^4_{n,N,M} =$$

$$= \frac{1}{2\pi} \sum_{|s|<M} (1 - \frac{|s|}{M}) \left\{ 2 \sum_j e^{-\mathrm{i}st_j} \delta^2_j(p) \left(\sum_h e^{\mathrm{i}st_h} \varepsilon^2_h + 2 \sum_h D_N(t_{h+1} - t_h) e^{\mathrm{i}st_h} \varepsilon_h \varepsilon_{h+1} \right) \right. \quad (25)$$

$$+\left(\sum_j e^{-\mathrm{i}st_j}(\varepsilon_j^2+2\delta_j(p)\varepsilon_j)\right)\left(\sum_h e^{\mathrm{i}st_h}(\varepsilon_h^2+2\delta_h(p)\varepsilon_h)\right) \tag{26}$$

$$+4\left(\sum_{j<j'} D_N(t_{j'}-t_j)e^{-\mathrm{i}st_{j'}}(\varepsilon_j\varepsilon_{j'}+2\delta_j(p)\varepsilon_{j'})\right)\left(\sum_{h<h'} D_N(t_{h'}-t_h)e^{\mathrm{i}st_{h'}}(\varepsilon_h\varepsilon_{h'}+2\delta_h(p)\varepsilon_{h'})\right) \tag{27}$$

$$+2\left(\sum_j e^{-\mathrm{i}st_j}(\varepsilon_j^2+2\delta_j(p)\varepsilon_j)\sum_{h<h'} D_N(t_{h'}-t_h)e^{\mathrm{i}st_{h'}}(\varepsilon_h\varepsilon_{h'}+2\delta_h(p)\varepsilon_{h'})\right)\Bigg\}. \tag{28}$$

Using the assumptions **(A.II)** and **(A.III)**:

$$E[\varepsilon_*^4]=2E[\eta^4]+6E[\eta^2]^2,\quad E[\delta_*(p)^2\varepsilon_*^2]=E[\delta_*(p)^2]2E[\eta^2],$$

$$E[\varepsilon_j^2\varepsilon_h^2]=4E[\eta^2]^2 \text{ if } |j-h|>1,\quad E[\varepsilon_j^2\varepsilon_h^2]=E[\eta^4]+3E[\eta^2]^2 \text{ if } |j-h|=1,$$

$$E[\varepsilon_j^3\varepsilon_h]=-(E[\eta^4]+3E[\eta^2]^2) \text{ if } |j-h|=1.$$

Consider (25). Except for the sum in the s index, its expectation is equal to:

$$2\sum_j e^{-\mathrm{i}st_j}E[\delta_j^2(p)]\left(\sum_h e^{\mathrm{i}st_h}2E[\eta^2]+2\sum_h D_N(\frac{2\pi}{n})e^{\mathrm{i}st_h}(-E[\eta^2])\right)$$

$$=4E[\eta^2]\,(1-D_N(\frac{2\pi}{n}))\sum_{j,h} e^{-\mathrm{i}s(t_j-t_h)}E[\delta_j^2(p)].$$

We can write (26) as

$$\sum_j(\varepsilon_j^4+4\delta_j(p)^2\varepsilon_j^2+2e^{-\mathrm{i}s(t_j-t_{j+1})}\varepsilon_j^2\varepsilon_{j+1}^2)+2\sum_{j+1<h} e^{-is(t_j-t_h)}\varepsilon_j^2\varepsilon_h^2,$$

therefore we get the following expectation

$$2n(1+e^{-\mathrm{i}s\frac{2\pi}{n}})(E[\eta^4]+3E[\eta^2]^2)+8E[\eta^2]\sum_j E[\delta_j(p)^2]+2\sum_{j+1<h} e^{-\mathrm{i}s(t_j-t_h)}4E[\eta^2]^2. \tag{29}$$

Consider (27). This is equal to

$$8D_N^2(\frac{2\pi}{n})\sum_{j<h} e^{-\mathrm{i}s(t_{j+1}-t_{h+1})}\varepsilon_j\varepsilon_{j+1}\varepsilon_h\varepsilon_{h+1}+4\sum_{j<j'} D_N^2(t_{j'}-t_j)\varepsilon_j^2\varepsilon_{j'}^2 \tag{30}$$

$$+8\sum_{j<j'} D_N(t_{j'}-t_j)D_N(t_{j'+1}-t_j)e^{-\mathrm{i}s(t_{j'}-t_{j'+1})}\varepsilon_j^2\varepsilon_{j'}\varepsilon_{j'+1}$$

$$+16\sum_{j<h',j'} D_N(t_{j'}-t_j)D_N(t_{h'}-t_j)e^{-\mathrm{i}s(t_{j'}-t_{h'})}\delta_j(p)^2\varepsilon_{j'}\varepsilon_{h'}.$$

Finally the expectation of (27) is computed as

$$8\;E[\eta^2]^2\;\sum_{j,h} D_N(t_{j+1}-t_j)D_N(t_{h+1}-t_h)e^{-\mathrm{i}s(t_{j+1}-t_{h+1})} \tag{31}$$

$$+4(E[\eta^4]+3E[\eta^2]^2)\ \sum_j D_N^2(t_{j+1}-t_j)+16\ E[\eta^2]^2\sum_{j'>j+1} D_N^2(t_{j'}-t_j)$$
$$-16E[\eta^2]^2\sum_{j<j'} D_N(t_{j'}-t_j)D_N(t_{j'+1}-t_j)e^{-\mathrm{i}s(t_{j'}-t_{j'+1})}$$
$$+16E[\eta^2]\sum_{j<j'}\left(D_N^2(t_{j'}-t_j)-D_N(t_{j'}-t_j)D_N(t_{j'+1}-t_j)e^{-\mathrm{i}s(t_{j'}-t_{j'+1})}\right)2E[\delta_j^2(p)].$$

Consider (28).

$$4\sum_{j<h} e^{-\mathrm{i}s(t_j-t_{h+1})}D_N(t_{h+1}-t_h)\varepsilon_j^2\varepsilon_h\varepsilon_{h+1}+4\sum_{j<h} e^{-\mathrm{i}s(t_j-t_h)}D_N(t_h-t_j)\varepsilon_j^3\varepsilon_h+ \tag{32}$$
$$+8\sum_j e^{-\mathrm{i}s(t_j-t_{j+1})}D_N(t_{j+1}-t_j)\delta_j^2(p)\varepsilon_j\varepsilon_{j+1}$$

Thus its mean is

$$-8E[\eta^2]^2\sum_{j<h} e^{-\mathrm{i}s(t_j-t_{h+1})}D_N(t_{h+1}-t_h)-4(E[\eta^4]+3E[\eta^2]^2)\sum_j e^{-\mathrm{i}s(t_{j+1}-t_j)}D_N(\frac{2\pi}{n})$$
$$-8\sum_j e^{-\mathrm{i}s(t_j-t_{j+1})}D_N(t_{j+1}-t_j)E[\eta^2]E[\delta_j^2(p)].$$

Therefore, rearranging terms and summing up on $|s|<M$, we can write

$$E[\widetilde{\sigma}^4_{n,N,M}-\sigma^4_{n,N,M}]=A_1+A_2+A_3$$

where

$$A_1\cong \operatorname{ess\,sup}\|\sigma^2\|_{L^\infty}\ 8\,E[\eta^2]\ \left(M(1-V_M(\frac{2\pi}{n}))+MV_M(\frac{2\pi}{n})(1-D_N(\frac{2\pi}{n}))\right.$$
$$\left.+\frac{2}{\pi}\ \frac{nM}{2N+1}(1-V_M(\frac{2\pi}{n}))+\frac{1}{4\pi}n(1-D_N(\frac{2\pi}{n}))\right).$$

The last terms goes to zero with the same conditions as in the theorem without noise.

$$A_2=\frac{2}{\pi}E[\eta^2]^2(\frac{n}{2\pi})^2M\left[\frac{2\pi^2}{M}2\left(1-2D_N(\frac{2\pi}{n})+D_N^2(\frac{2\pi}{n})\right)+\frac{(2\pi)^2}{2N+1}\left(4-4V_M(\frac{2\pi}{n})\right)\right]$$
$$=\frac{1}{\pi}E[\eta^2]^2n^2\left((1-D_N(\frac{2\pi}{n}))^2+8\frac{M}{2N+1}(1-V_M(\frac{2\pi}{n}))\right).$$

This term goes to zero as $\frac{N^2}{n}\to 0$ and $\frac{M^3}{N}\to 0$.

Finally

$$A_3=\frac{1}{\pi}(E[\eta^4]+3E[\eta^2]^2)\ nM\left(1+V_M(\frac{2\pi}{n})+2D_N^2(\frac{2\pi}{n})-2D_N(\frac{2\pi}{n})V_M(\frac{2\pi}{n})\right)$$
$$=\frac{1}{\pi}(E[\eta^4]+3E[\eta^2]^2)\left(nM(1-V_M(\frac{2\pi}{n}))+2nMV_M(\frac{2\pi}{n})(1-D_N(\frac{2\pi}{n}))\right) \tag{33}$$
$$+\frac{1}{\pi}(E[\eta^4]+3E[\eta^2]^2)\left(nM2D_N^2(\frac{2\pi}{n})\right). \tag{34}$$

The term (33) goes to zero as $\frac{M^3}{n}\to 0$ and $\frac{MN^2}{n}\to 0$, while (34) diverges. Finally, except for a diverging term (34), we have proved that $E[\widetilde{\sigma}^4_{n,N,M}-\sigma^4_{n,N,M}]$ converges to 0 under the given growth conditions. □